

Supporting Information

Ahp-Cyclodepsipeptides as tunable inhibitors of human neutrophil elastase and kallikrein 7: total synthesis of tutuilamide A, serine protease selectivity profile and comparison with lymbyastatin7

Qi-Yin Chen^{a,b,1}, Danmeng Luo^{a,b,1}, Gustavo M. Seabra^{a,b}, Hendrik Luesch^{a,b*}

^aDepartment of Medicinal Chemistry, University of Florida, Gainesville, Florida 32610, United States

^bCenter for Natural Products, Drug Discovery and Development (CNP3), University of Florida, Gainesville, Florida 32610, United States

Corresponding author: luesch@cop.ufl.edu (H. Luesch)

¹These authors contributed equally to this work.

Content

1. Table S1. Comparison of NMR data for natural and synthetic tutuilamide A	Page 2-3
2. Table S2. Reaction conditions for protease assays	Page 4
3. Supplementary material for docking	Page 5
4. Table S3. Details of the docking results	Page 6
5. Figure S2. Sequence alignment of PPE, HNE, and KLK7	Page 6
6. Figure S3. Results from redocking validation experiments (PPE)	Page 7
7. Figure S4. Results from cross-docking validation experiments (PPE)	Page 8
8. Figure S5. Ligand interaction diagrams (HNE, KLK7)	Page 9
9. Figure S6. Positioning of Arg217 (HNE)	Page 10
10. NMR spectra of intermediates 4-7	Page 11-16
11. Comparison of NMR spectra of synthetic tutuilamide A (1) and natural tutuilamide A	Page 17-18

Table S1. Comparison of NMR data for natural and synthetic tutuilamide A in DMSO-*d*₆ (*J* in Hz)

AA	C/H no	δ_{H} (<i>J</i> in Hz)		δ_{C}	
		Nat/500 MHz	Syn/600 MHz	Nat/125 MHz	Syn/150 MHz
Val	1			170.8 ^b , C	170.5, C
	2	4.65, o	4.64, br m	56.1, CH	56.2, CH
	3	2.07, dq (12.1, 6.8)	2.06, dq (13.3, 7.0)	30.5, CH	30.7, CH
	4	0.88, d (6.8)	0.87, d (6.8)	18.9, CH ₃	19.2, CH ₃
	5	0.75, d (6.8)	0.76, d (6.8)	17.3, CH ₃	17.5, CH ₃
	NH	7.53, t (9.5)	7.51, d (8.2)		
Tyr	1			169.2, C	169.4, C
	2	4.89, dd (11.5, 2.2)	4.89, dd (11.0, 3.0)	60.8, CH	60.8, CH
	3a	3.11, dd (14.5, 2.2)	3.09, dd (14.5, 2.7)	32.5, CH ₂	32.8, CH ₂
	3b	2.69,, dd (14.3, 11.9)	2.70,, dd (14.4, 11.5)		
	4			127.3, C	127.4, C
	5	7.00, d (8.3)	6.99, d (8.4)	130.2, CH	130.4, CH
	6	6.78, d (8.3)	6.76, d (8.5)	115.3, CH	115.3, CH
	7			156.1, C	156.2, C
N-Me	2.77, s	2.76, s	30.2, CH ₃	30.4, CH ₃	
Phe	1			170.2 ^b , C	170.5, C
	2	4.73, dd (11.4, 4.0)	4.73, dd (11.5, 4.5)	50.2, CH	50.2, CH
	3a	2.88, o	2.87, dd (13.8, 11.4)	35.2, CH ₂	35.3, CH ₂
	3b	1.83, dd (13.8, 11.7)	1.81, br m		
	4			136.5, C	136.7, C
	5	6.83, d (7.2)	6.83, d (7.1)	129.2, CH	129.4, CH
	6	7.18, t (7.2)	7.19, t (7.3)	127.5, CH	127.8, CH
	7	7.15, t (7.2)	7.15, t (7.2)	126.2, CH	126.2, CH
Ahp	1			168.5, C	168.7, C
	2	3.79, m	3.78, m	48.2, CH	48.2, CH
	3a	2.42, m	2.42, m	21.9, CH ₂	21.9, CH ₂
	3b	1.58, m	1.57, br m		
	4a	1.72, o	1.71, br m	29.2, CH ₂	29.4, CH ₂
	4b	1.58, o	1.57, br m		
	5	5.08, b	5.08, br t (2.4)	73.7, CH	73.7, CH
	NH	7.22, b	7.21, br		
	OH	6.15	—		
Abu	1			162.6, C	162.9, C
	2			129.9, C	130.0, C
	3	6.52, q (7.0)	6.51, q (7.1)	131.5, CH	131.6, CH
	4	1.48, d (7.1)	1.48, d (7.1)	13.0, CH ₃	13.0, CH ₃
	NH	9.23, b	9.16, br		

Table S1 (continued)

AA	C/H no	δ_{H} (<i>J</i> in Hz)		δ_{C}	
		Nat/500 MHz	Syn/600 MHz	Nat/125 MHz	Syn/150 MHz
Thr	1			172.4, C	172.7, C
	2	4.67, o	4.65, br m	55.1, CH	55.2, CH
	3	5.53, b	5.51, br	71.7, CH	71.7, CH
	4	1.21, d (6.6)	1.21, d (6.5)	17.8, CH ₃	18.0, CH ₃
	NH	7.91, b	7.89, br		
Ile	1			171.6, C	171.9, C
	2	4.40, t (7.8)	4.39, dd (7.6, 7.6)	56.5, CH	56.7, CH
	3	1.81, o	1.81, br m	36.5 ^c , CH	40.1 ^c , CH
	4a	1.43, o	1.41, m	23.9, CH ₂	24.0, CH ₂
	4b	1.08, o	1.07, m		
	5	0.80, t (7.5)	0.80, t (7.4)	11.0, CH ₃	11.1, CH ₃
	6	0.84, d (6.8)	0.84, d (6.8)	15.3, CH ₃	15.3, CH ₃
	NH	7.85, b	7.82, br		
Ala	1			172.0, C	172.2, C
	2	4.36, p (7.2)	4.35, dq (7.2)	48.2, CH	48.1, CH
	3	1.19, d (7.0)	1.19, d (7.1)	17.9, CH ₃	18.0, CH ₃
	NH	8.21, d (7.4)	8.18, d (7.5)		
Cmb	1			168.4, C	168.6, C
	2	2.97, s	2.96, s	42.5, CH ₂	42.6, CH ₂
	3			133.9, C	134.1, C
	4	6.10, d (1.1)	6.11, q (1.3)	114.3, CH	114.3, CH
	5	1.72, d (1.2)	1.72, d (1.3)	16.3, CH ₃	16.4, CH ₃

Note: ^bOriginal ¹³C NMR spectrum of natural product shows same chemical shift at about 170.5 ppm for these two carbons; ^cBoth ¹³C NMR spectra of natural and synthetic tutuilamide A do not show a signal at 36.5 ppm, probably the peak at 40.1 ppm is the signal of this carbon.

Table S2. Reaction conditions for protease assays

Protease	Enzyme Source	Substrate	Sub in RXN (μ M)	Ex/Em (nm)	buffer/ Co-Factor
Cathepsin G	Human neutrophil	Suc-AAPF-AMC	10	355/460	Buffer C
Chymase	Human skin	Suc-AAPF-AMC	10	355/460	Buffer C
Chymotrypsin	Bovine pancreas	Suc-AAPF-AMC	10	355/460	Buffer C
Elastase	Human Neutrophil	MeOSuc-AAPV-AMC	10	355/460	B
Factor VIIa	Human plasma	Z-VVR-AMC	10	355/460	Buffer A
Factor Xa	Human plasma	CH ₃ SO ₂ -D-CHA-Gly-Arg-AMC-AcOH	10	355/460	E
Factor XIa	Human plasma	(Boc-Glu(OBzl)-Ala-Arg)-MCA	10	355/460	Buffer A
Kallikrein 1	Human recombinant aa25-262	Z-VVR-AMC	10	355/460	F
Kallikrein 5	Human recombinant aa67-293	Z-VVR-AMC	10	355/460	Buffer A
Kallikrein 7	Human recombinant aa23-252	MCA-RPKPVE-Nval-WRK(Dnp)-N	10	320/405	G
Kallikrein 12	Human recombinant aa18-248	BOC-VPR-AMC	10	380/460	H
Kallikrein 13	Human recombinant aa1-262	BOC-VPR-AMC	10	380/460	I
Kallikrein 14	Human recombinant aa19-248	BOC-VPR-AMC	10	380/460	J
Matriptase-2	Human recombinant aa 78-811	Boc--Gln-Ala-Arg-AMC	10	355/460	K
Plasma Kallikrein	Human recombinant aa20-638	Z-FR-AMC	10	380/460	L
Plasmin	Human plasma	H-D-CHA -Ala-Arg-AMC.2AcOH	10	355/460	Buffer A
Proteinase A	Bacillus licheniformis	Z-GPR-AMC	10	355/460	Buffer A
Proteinase K	Tritirachium album limber	H-D-CHA -Ala-Arg-AMC.2AcOH	10	355/460	Buffer A
TACE	Human recombinant aa215-671	MCA-PLAQAV-Dpa-RSSSR-NH ₂	10	320/405	Buffer F
Thrombin alpha	Human plasma	H-D-CHA -Ala-Arg-AMC.2AcOH	10	355/460	M
Trypsin	Bovine pancreas	H-D-CHA -Ala-Arg-AMC.2AcOH	10	355/460	Buffer A
Tryptase beta 2	Human recombinant	Z-GPR-AMC	10	355/460	N
Tryptase gamma 1	Human lung	Z-GPR-AMC,	10	355/460	Buffer A
Urokinase	Human urine	Bz-b-Ala-Gly-Arg-AMC.AcOH	10	355/460	Buffer A

Buffer/Co-factor

A: 25 mM Tris pH 8.0, 100 mM NaCl, 0.01% Brij35,

B: 50 mM Tris, pH 7.5, 1 M NaCl, 0.05 % Brij35

C: 100 mM Tris-HCl, pH 8.0, 50 mM NaCl, 10 mM CaCl₂, 0.025% CHAPS, 1.5 mM DTT

D: 50 mM Tris, 150 mM NaCl, pH 8.5

E: 25 mM Tris pH 7.5, 10 mM CaCl₂, 150 mM NaCl, 0.05% Brij35

F: 25 mM Tris pH 9, 2.5 μ M ZnCl₂, 0.005% Brij

G: Activate 0.1mg/ml with 10ug/ml Thermolysin in buffer E for 1h 37°C, 50mM EDTA to stop, buffer D

H: AutoActivate 100 μ g/ml in 0.1M Tris pH 8, CNB 16h at 37°C, buffer E

I: Activate 100 μ g/ml with 0.02 μ g/ml Lysyl Endopeptidase in 0.1M Tris pH 8, 30min at 37°C, buffer A

J: Activate 0.1 mg/ml with 10 μ g/ml Thermolysin in buffer E for 1h 37°C, 50 mM EDTA to stop, buffer A

K: 100mM TRIS, pH 9.0, 0.5 mg/ml BSA

L: Activate 0.1mg/ml with 10 μ g/ml Thermolysin in TCN for 30min 37°C, 10mM EDTA to stop, buffer A

M: Buffer A + 2.5 mM CaCl₂ + 1 mg/ml BSA

N: Unstable w/o 2M NaCl, dilute immediately before, buffer A

Supplementary Material for Docking

Validation

Two strategies were used to validate the chosen strategy. First, the tutuilamide A and lyngbyastatin 7 ligands were docked to PPE from their original structure (redocking), which evaluates the capacity of the program to reproduce the original structure. Then they were each docked to the other structure (cross-docking), to evaluate the capacity to find a good pose for the ligand in a different structure. In both cases the structure obtained for the ligand was compared to the original one by RMSD on the heavy atoms.

Redocking. Figure S2 shows the lowest scoring structures obtained from the redocking experiments, and the corresponding energies and RMSD to the original structures are in Table S3. The docked tutuilamide A structure is very similar to the experimental one (6TH7), with RMSD of only 1.192 Å. The major differences between docked and crystal structures are in a slight rotation of the Tyr phenol ring which makes a T-shaped $\pi - \pi$ interaction to Phe, and which is normally solvent exposed, not affecting binding. As in the crystal structure, the Ahp forms one H-bond between the carbonyl and PPE Gln191 and two intramolecular H-bonds, one from the hydroxyl Val-NH and another between the amino-N and Thr carbonyl. Tutuilamide A cyclic structure also interacts with PPE through H-bonds between the Abu carbonyl and Gly192 and Ser194, Abu-N and Ser213. In the linear chain, the Ile forms 2 H-bonds to Val215, and Arg217 makes 2 H-bond to tutuilamide A, to the Ala and Cmb carbonyls.

As for L7 docked into the 4GVU structure, the docked structure is again very similar to the crystallographic (4GVU) pose, with RMSD 1.35 Å. The main difference is a movement from Gln2, which breaks the original intramolecular H-bond to the Tyr carbonyl to form an H-bond to Ser216 backbone. The cyclic structure in lyngbyastatin 7 makes the same interactions as in tutuilamide A, and the Gln in the linear chain forms 3 H-bond to PPE, being two to Val215 and one to Ser216. Arg217 is too far to form any bond.

Cross Dockings. We also did cross-dockings experiments following the same procedure, where tutuilamide A was docked to the PPE structure obtained in the presence of lyngbyastatin 7 (4GVU), and also docking lyngbyastatin 7 in the PPE structure obtained in the presence of tutuilamide A (6TH7). The obtained structures are depicted in Figure S3. In both cases, the structure with best SP docking score had an RMSD to the original structure below 2.0 Å (Table S3). The structure of tutuilamide A docked to 4GVU has an RMSD of only 1.548 Å to the tutuilamide A crystal structure (6TH7). The main difference is in the Tyr ring which rotates, losing the $\pi - \pi$ interaction with Phe. Otherwise, the same bonds as present in 6TH7 are noticeable. The same happens with lyngbyastatin 7, which keeps the same bonds as in the redocking experiment. One difference is that, in the lyngbyastatin 7 case, the Tyr ring is in the same position and still forms the T-shaped stacking interaction with Phe.

Taken together, the results from redocking and cross-docking provide good confidence in the ability of the protocol to accurately describe the interactions between the cyclodepsipeptides and the proteins considered here.

Table S3. Details of the docking results. Energies are in kcal/mol, and RMSD in Å. RMSD values are calculated with respect to the crystal structures of tutuilamide A or lyngbyastatin 7 from the PDB (PDBIDs: 6TH7 and 4GVU, respectively).

Ligand	Target	PDBID	Glide SP		MM-GBSA	
			DockScore	RMSD	BE	RMSD
Tutuilamide A	PPE	6TH7	-10.12	1.49	-113.23	1.19
Tutuilamide A	PPE	4GVU	-9.28	1.65	-102.51	1.55
Tutuilamide A	HNE	3Q76	-7.58	3.28	-95.41	3.02
Tutuilamide A	KLK7	2QXI	-8.77	1.85	-93.79	1.60
Lynbyastatin 7	PPE	4GVU	-9.51	1.92	-111.38	1.35
Lynbyastatin 7	PPE	6TH7	-10.09	1.85	-104.83	1.87
Lynbyastatin 7	HNE	3Q76	-6.96	2.86	-74.17	2.16
Lynbyastatin 7	KLK7	2QXI	-9.65	1.58	-101.47	1.44

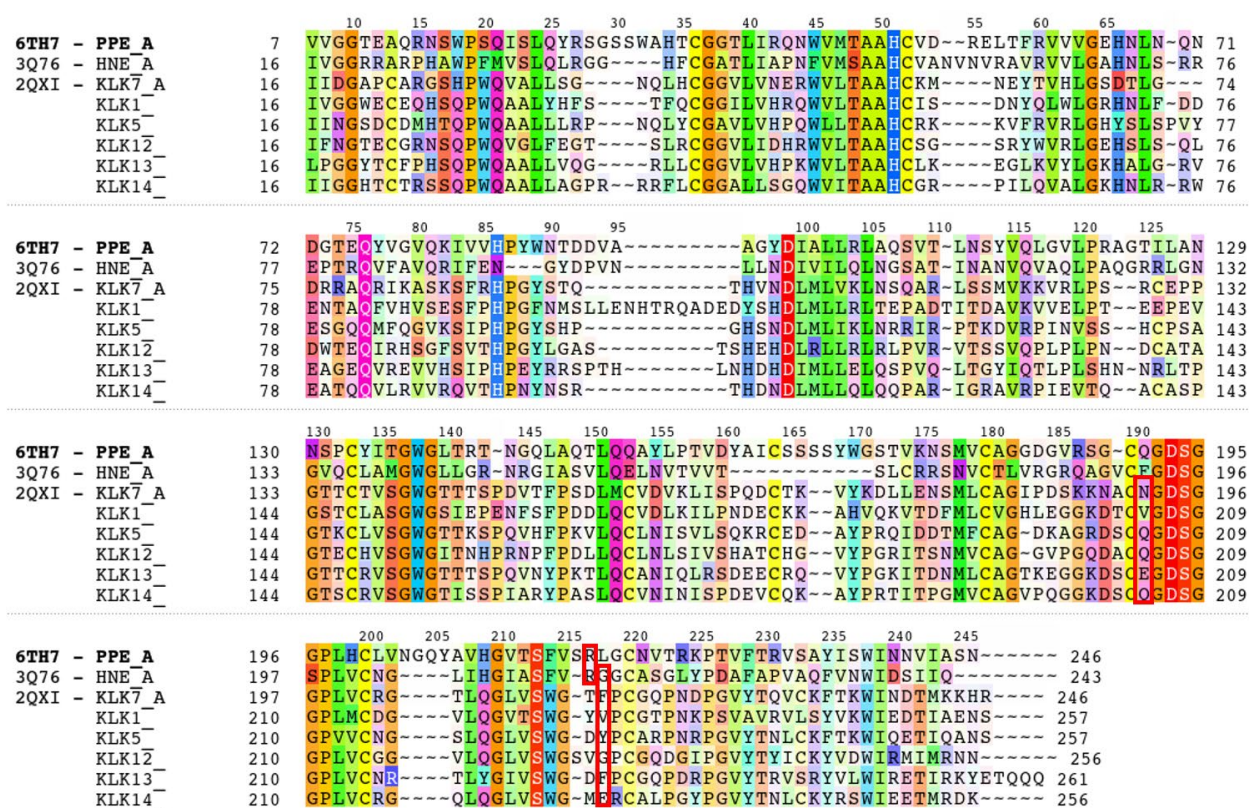


Figure S1. Sequence alignment of PPE, HNE, KLK7 and other human KLKs tested by protease profiling. Boxed residues are discussed in the text.

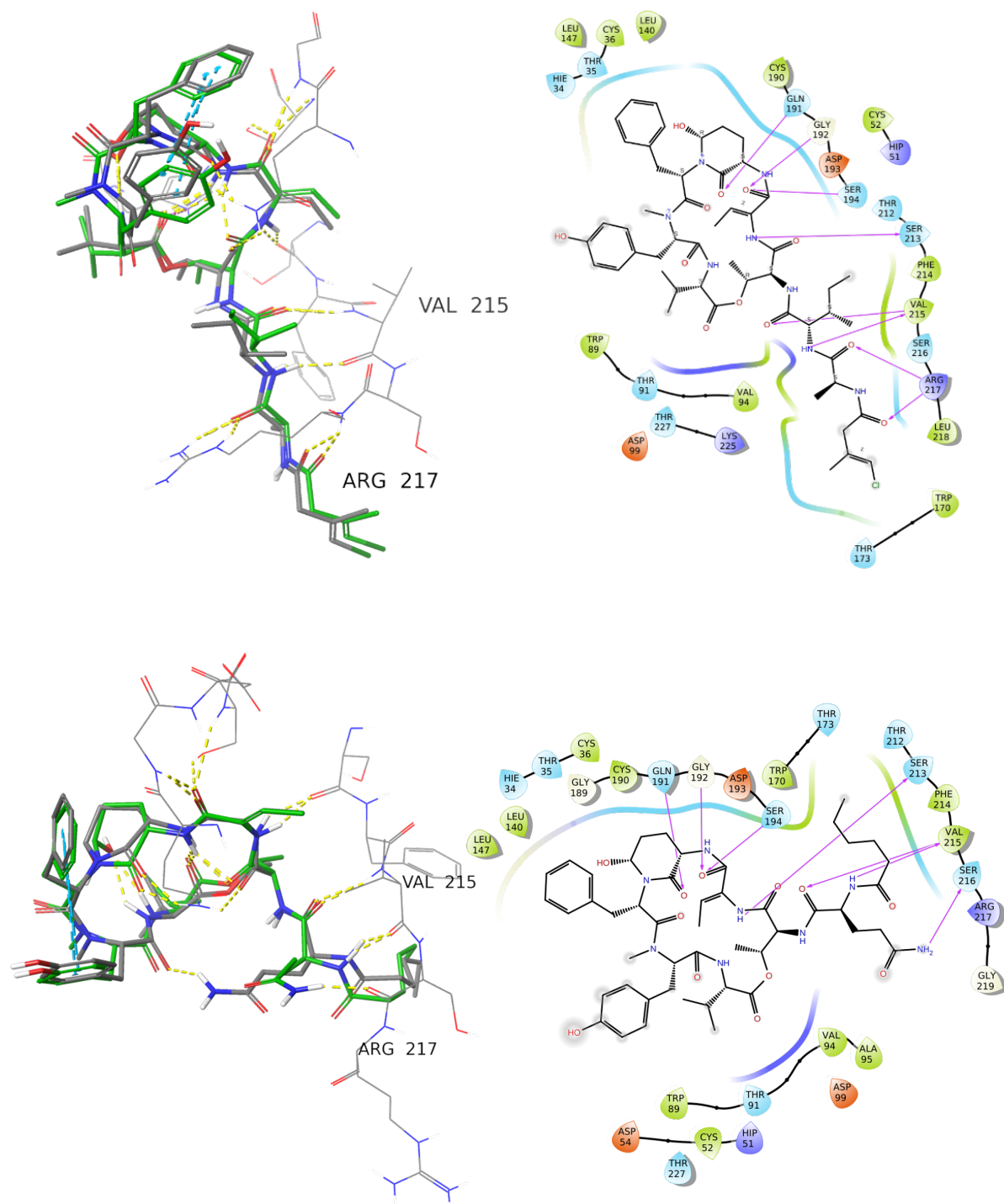


Figure S2. Results from redocking validation experiments. Top: tutuilamide A docked into PPE (6TH7). Bottom: lyngbyastatin 7 docked into PPE (4GVU). In both cases the docked structure is in green, and the original (crystal) structure in grey. On the right, the corresponding Ligand Interaction Diagrams. Purple arrows indicate hydrogen bonds.

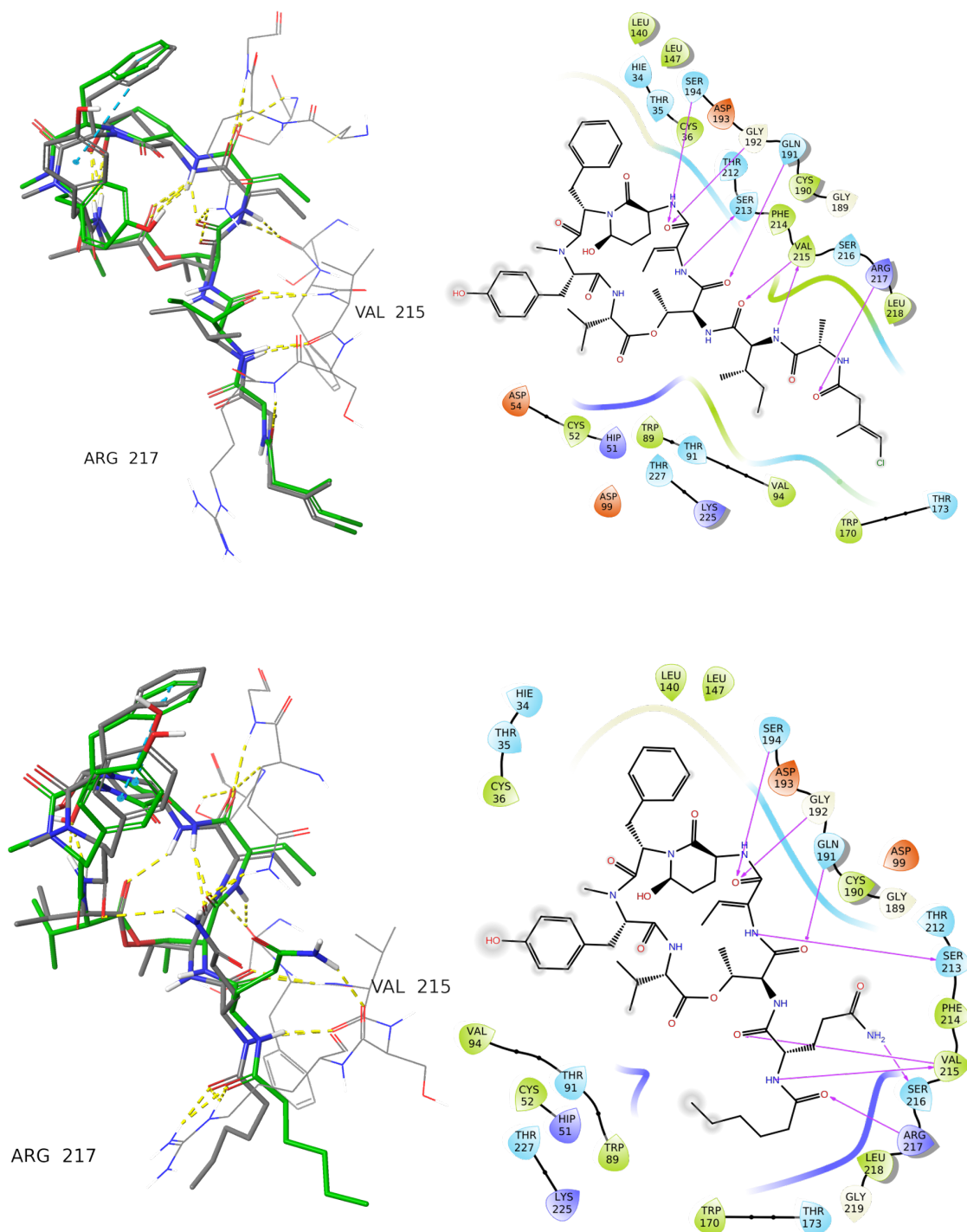


Figure S3. Results from cross-docking validation experiments. Top: tutuilamide A docked into PPE (4GVU). Bottom: lyngbyastatin 7 docked into PPE (6TH7). In both cases the docked structure is in green, and the original (crystal) structure in grey. On the right, the corresponding Ligand Interaction Diagrams. Purple arrows indicate hydrogen bonds

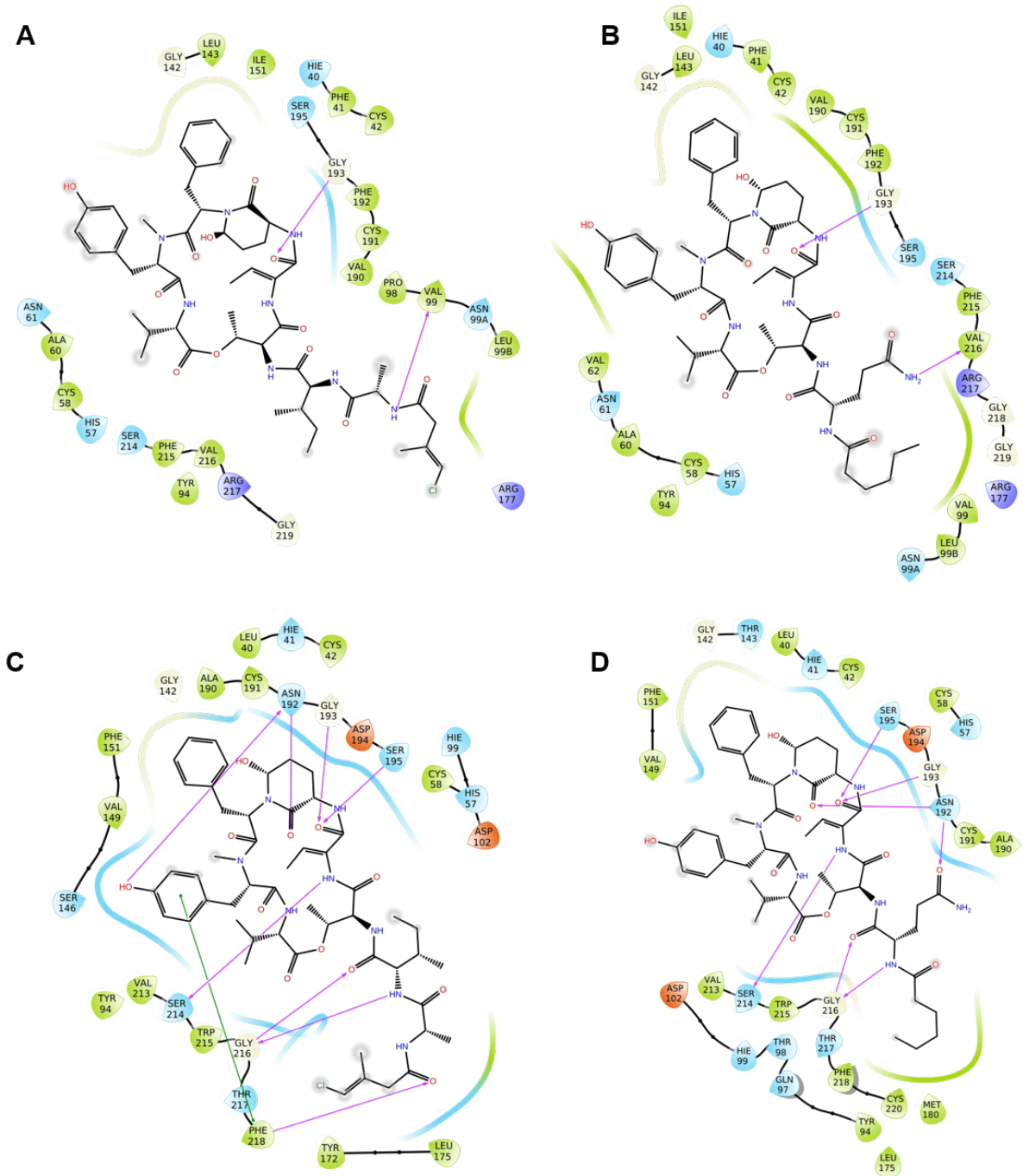


Figure S4. Ligand interaction diagrams depicting the most important interactions of tutuilamide A (A,C) and linybyastatin 7 (B,D) with HNE (top) and KLK7 (bottom). Purple arrows in the LIDs represent hydrogen bonds.

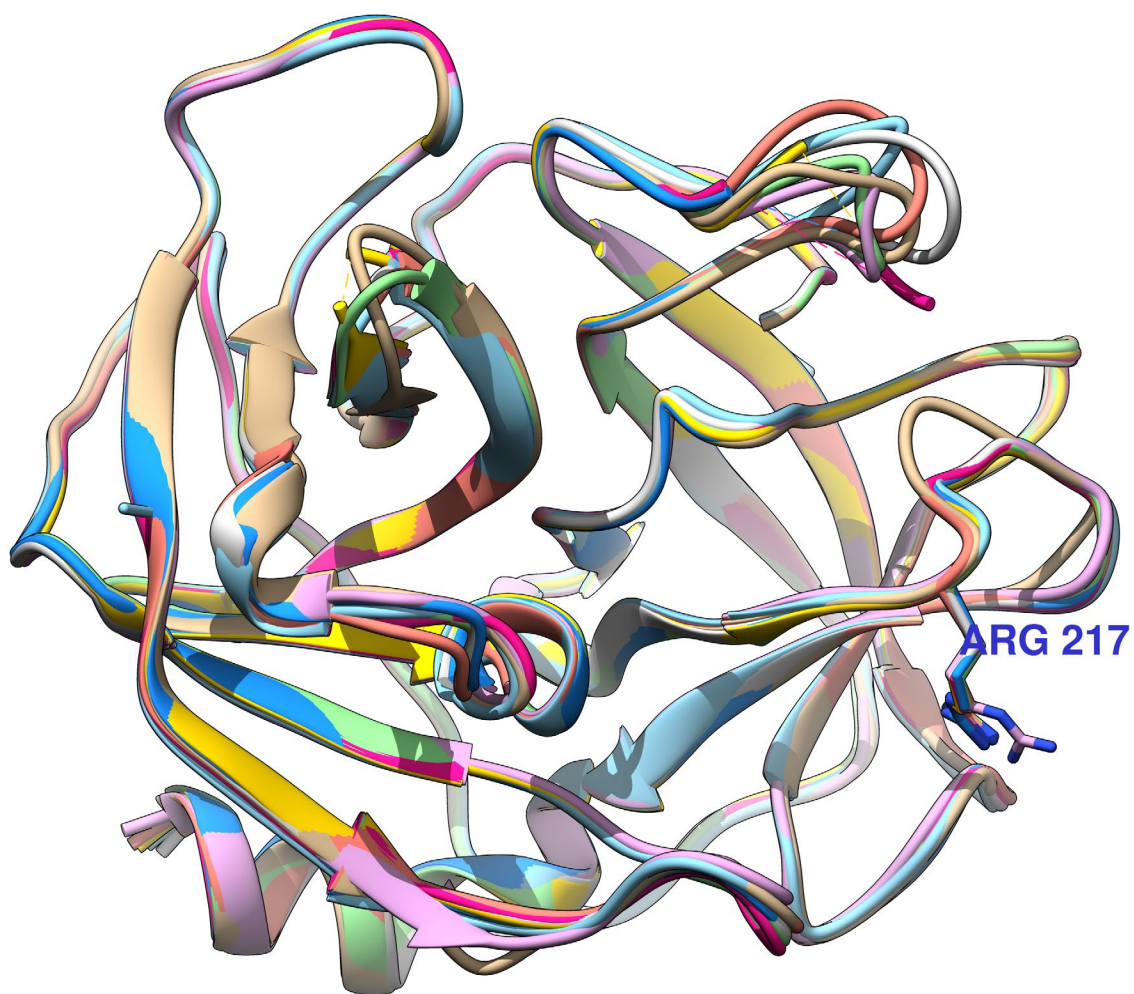


Figure S5. Positioning of Arg217 in a superposition of 9 different crystal structures for HNE (PDBIDs: 1HNE, 2Z7F, 5A0A, 5A09, 5A8Y, 3Q76, 3Q77, 4WVP, 5ABW).

Figure S6. ¹H NMR spectrum of compound 4 in CDCl₃ (600 MHz) at 27 °C.

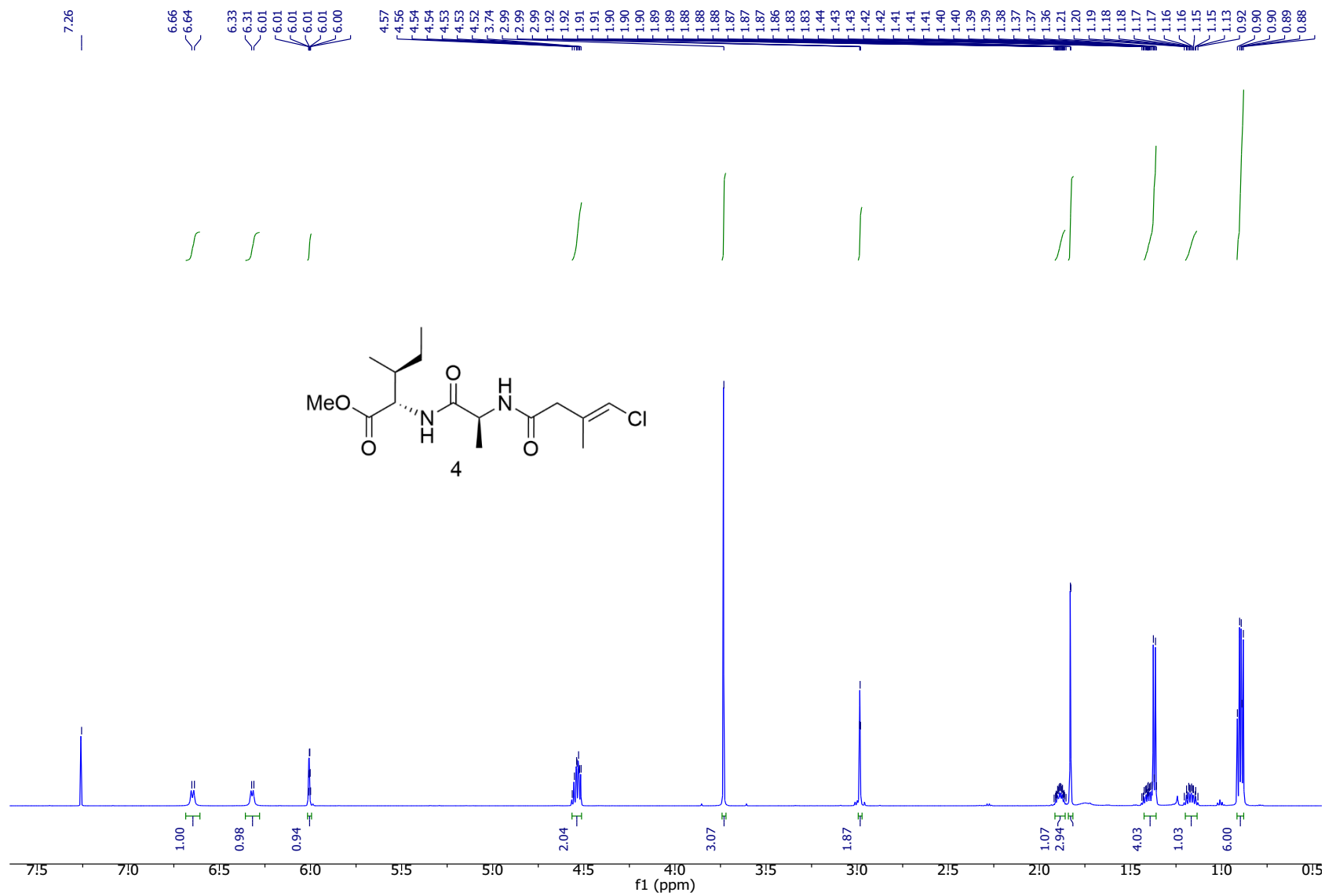


Figure S7. ^{13}C NMR spectrum of compound **4** in CDCl_3 (150 MHz) at 27 °C.

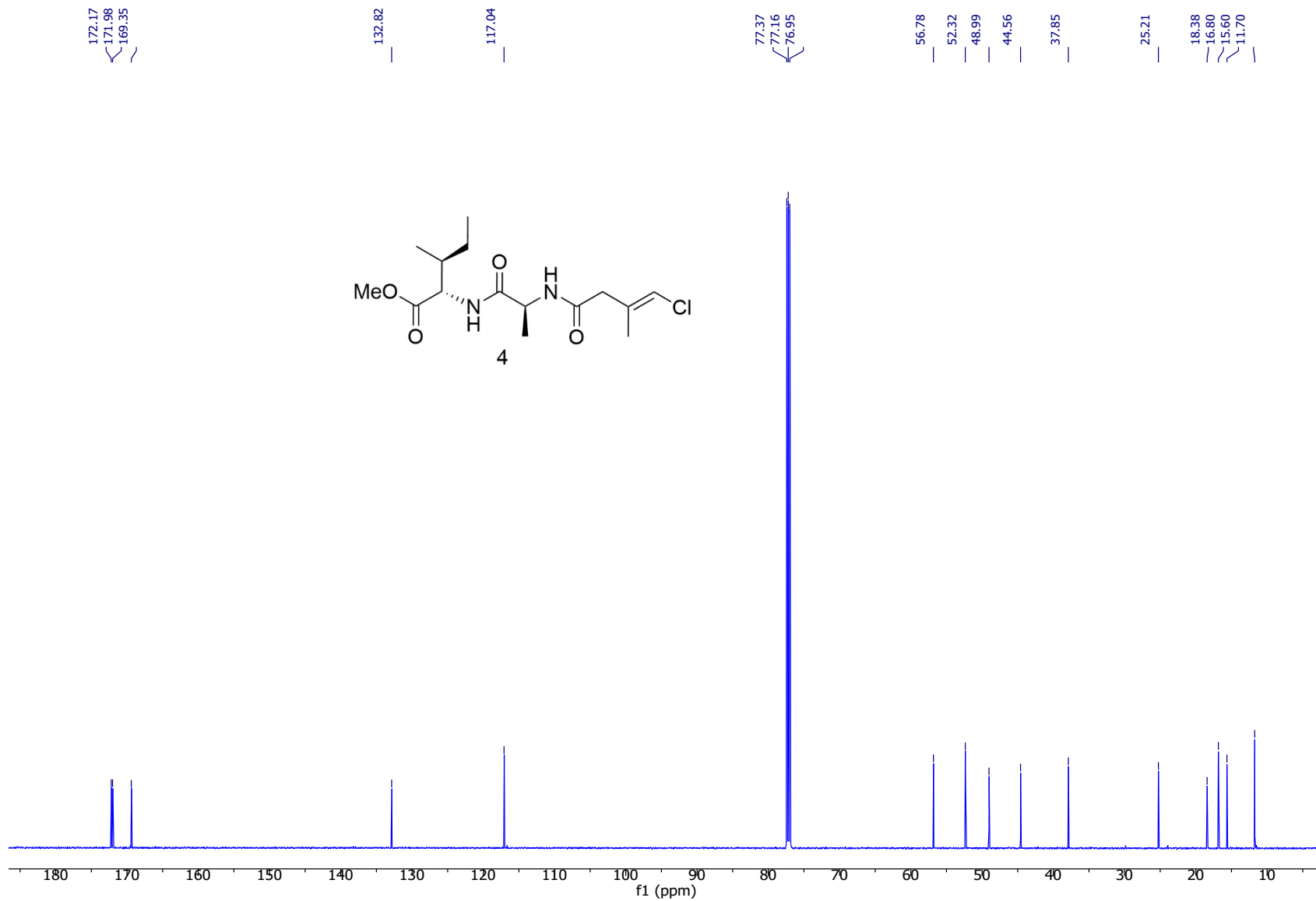


Figure S8. ¹H NMR spectrum of compound **5** in DMSO-*d*₆ (600 MHz) at 27 °C.

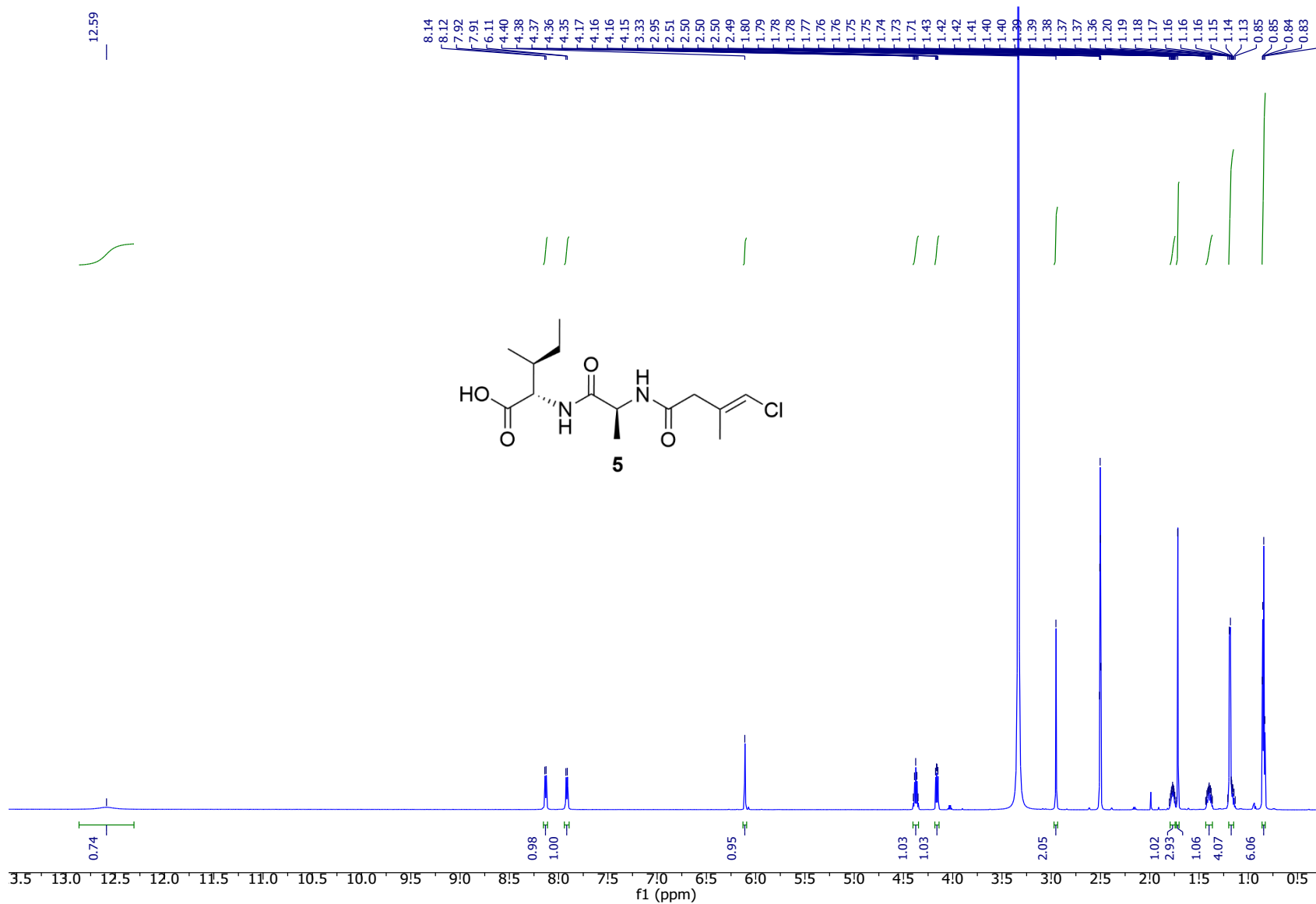


Figure S9. ^{13}C NMR spectrum of compound **5** in $\text{DMSO-}d_6$ (150 MHz) at 27 °C.

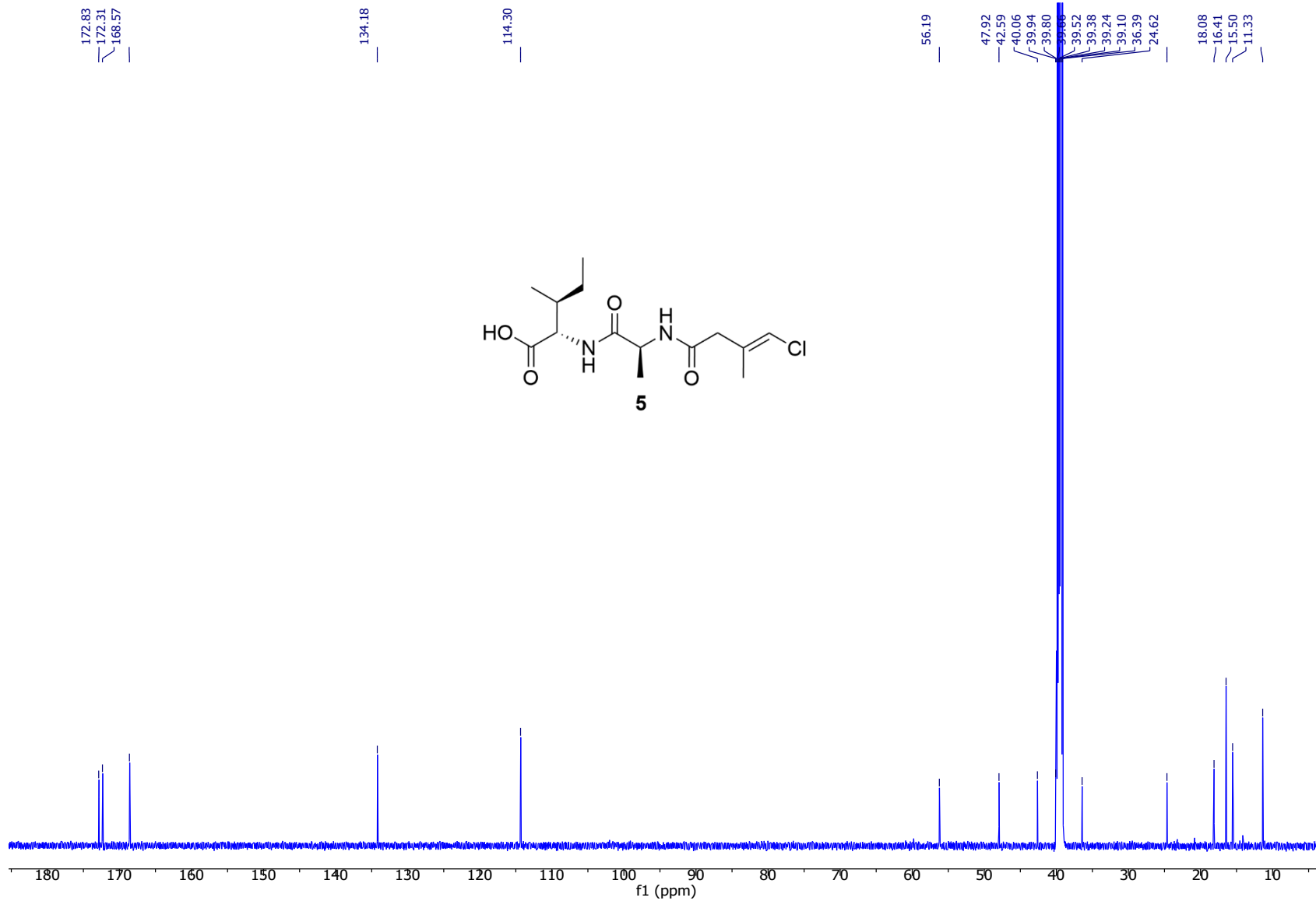


Figure S10. ^1H NMR spectrum of compound **7** in $\text{DMSO-}d_6$ (600 MHz) at 27 °C.

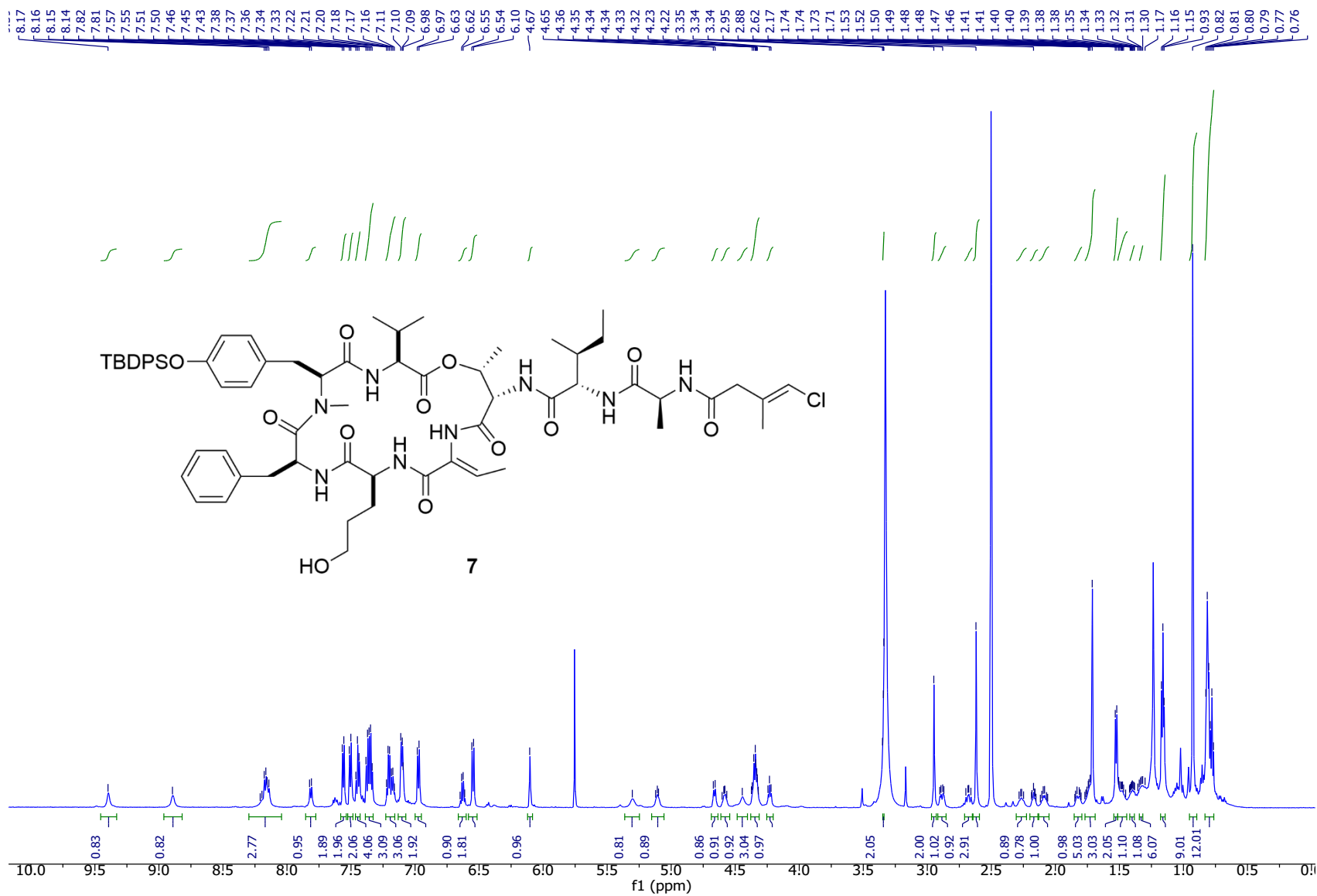


Figure S11. ^{13}C NMR spectrum of compound **7** in $\text{DMSO-}d_6$ (150 MHz) at 27 $^\circ\text{C}$.

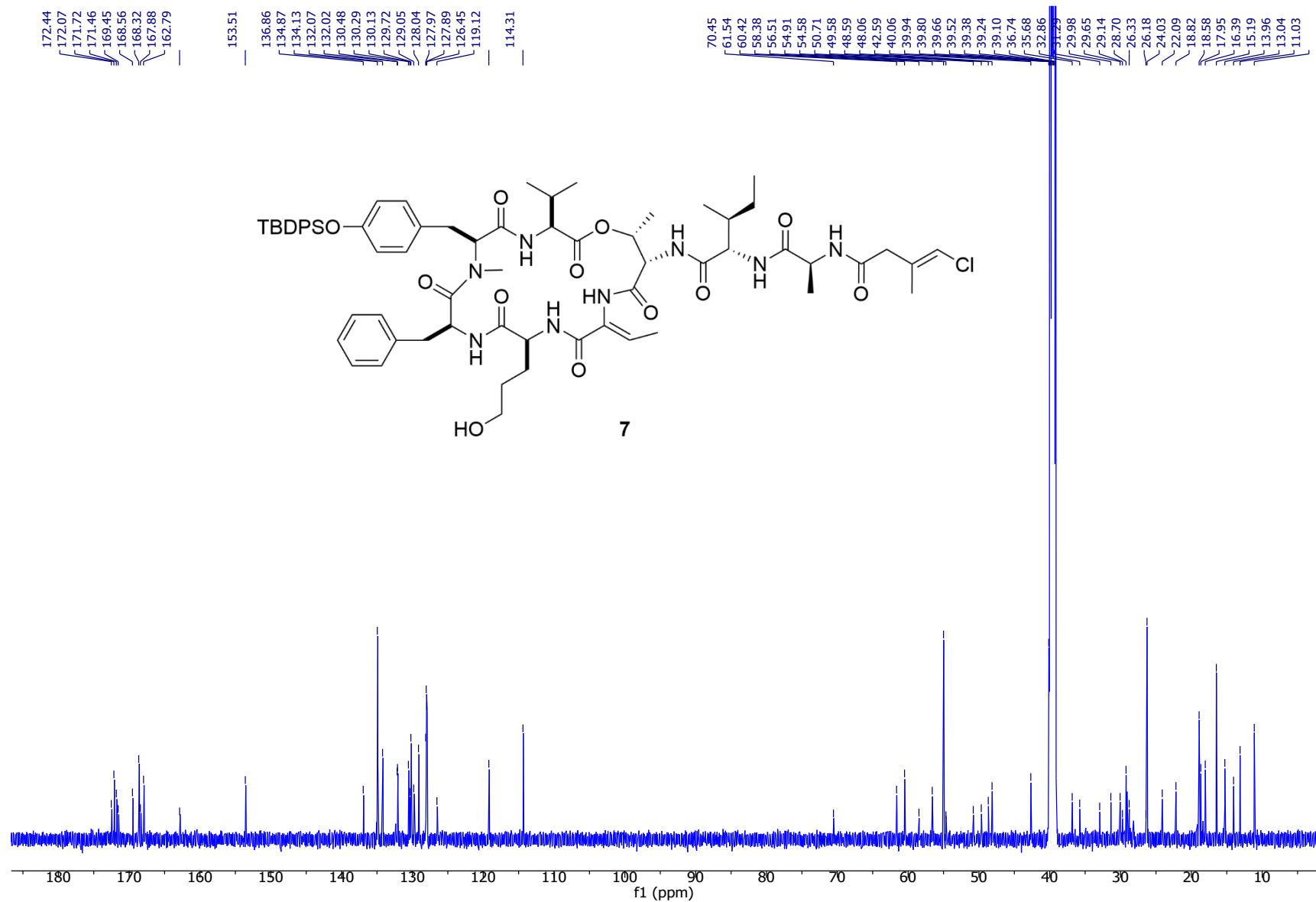


Figure S12. Comparison of ^1H NMR spectrum of synthetic tutuilamide A (**1**) (down) and natural tutuilamide A (up) in $\text{DMSO-}d_6$ (150 MHz) at 27 $^\circ\text{C}$.

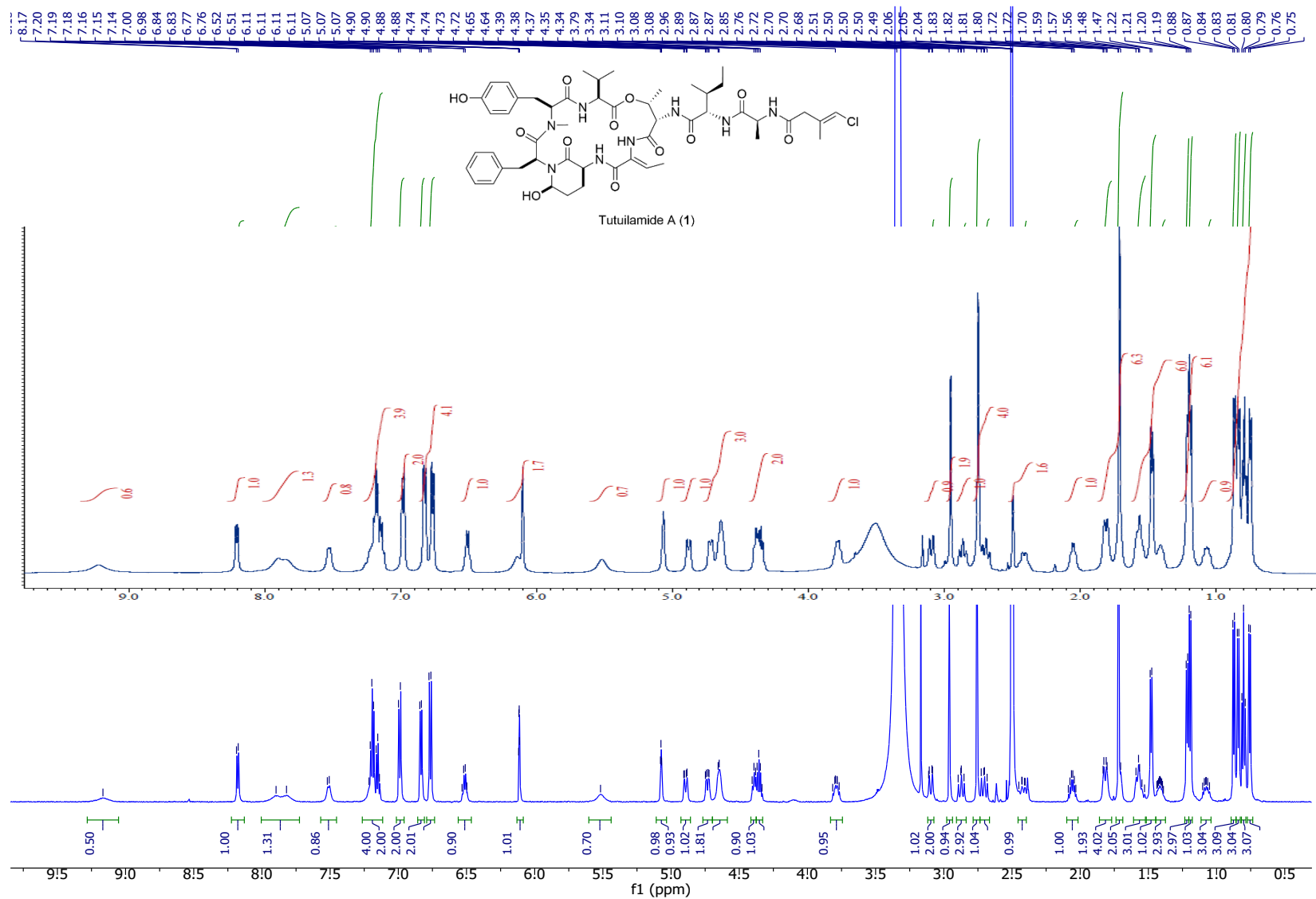


Figure S13. Comparison of ^{13}C NMR spectrum of synthetic tutuilamide A (**1**) (bottom) and natural tutuilamide A (top) in $\text{DMSO-}d_6$ (150 MHz) at 27 °C.

